AD-A088 094 NAVAL UNDERWATER SYSTEMS CENTER NEW LONDON CT NEW LO--ETC F/G 20/3
CALCULATION OF THE BIOT-SAVART LAW MAGNETIC FIELD USING CURRENT--ETC(U)
JUL 80 J W FRYE
UNCLASSIFIED NUSC-TR-6281 NL

1 OF 1
AD
A088094

END
DATE
FILMED
9-80
DTIC

LEVEL II

NUSC Technical Report 6281

NUSC Technical Report 6281

AD A088094

# Calculation of the Biot-Savart Law Magnetic Field Using Current Distributions Obtained From a Finite Element Analysis

John W. Frye
Office of Engineering Mechanics



27 July 1980

NUSC
Naval Underwater Systems Center
Newport, Rhode Island • New London, Connecticut





80 8 20 075

## Preface

This report was prepared under NUSC Project No. A53223, "Finite Element Modeling of Electric and Electromagnetic Fields" (U), Principal Investigator, R. G. Kasper (Code 401), and Associate Principal Investigator, J. W. Frye (code 401), Navy Subproject and Task No. B-0005, 11221; Naval Industrial Funding from David W. Taylor Naval Ship Research and Development Center, Project Director, W. Andahazy (DTNSRDC, Code 2704); Program Manager, W. L. Welsh (NAVMAT PM-2-21).

The Technical Reviewer for this report was M. Melehy, Code 401 (Professor of Electrical Engineering at the University of Connecticut).

**Reviewed and Approved: 27 July 1980**

**J. F. Kelly, Jr.**
**Head: Engineering and Technical**
**Support Department**

The author of this report is located at the New London Laboratory, Naval Underwater Systems Center, New London, Connecticut 06320.

14

NUSC-

# REPORT DOCUMENTATION PAGE

READ INSTRUCTIONS BEFORE COMPLETING FORM

| | | |
|---|---|---|
| 1. REPORT NUMBER<br>TR-6281 | 2. GOVT ACCESSION NO.<br>AD-A088094 | 3. RECIPIENT'S CATALOG NUMBER |
| 4. TITLE (and Subtitle)<br>6 CALCULATION OF THE BIOT-SAVART LAW MAGNETIC FIELD USING CURRENT DISTRIBUTIONS OBTAINED FROM A FINITE ELEMENT ANALYSIS. | | 5. TYPE OF REPORT & PERIOD COVERED<br>9 Technical rept.<br>6. PERFORMING ORG. REPORT NUMBER |
| 7. AUTHOR(s)<br>10 John W. Frye | | 8. CONTRACT OR GRANT NUMBER(s) |
| 9. PERFORMING ORGANIZATION NAME AND ADDRESS<br>Naval Underwater Systems Center<br>New London Laboratory<br>New London, CT 06320 | | 10. PROGRAM ELEMENT, PROJECT, TASK AREA & WORK UNIT NUMBERS<br>A53223 |
| 11. CONTROLLING OFFICE NAME AND ADDRESS<br>Naval Material Command (PM-2-21)<br>Washington, DC 20362 | | 12. REPORT DATE<br>11 27 Jul[redacted]80<br>13. NUMBER OF PAGES<br>26 |
| 14. MONITORING AGENCY NAME & ADDRESS(if different from Controlling Office)<br>12 31 | | 15. SECURITY CLASS. (of this report)<br>UNCLASSIFIED<br>15a. DECLASSIFICATION/DOWNGRADING SCHEDULE |

16. DISTRIBUTION STATEMENT (of this Report)

Approved for public release; distribution unlimited.

17. DISTRIBUTION STATEMENT (of the abstract entered in Block 20, if different from Report)

18. SUPPLEMENTARY NOTES

19. KEY WORDS (Continue on reverse side if necessary and identify by block number)

| | |
|---|---|
| Biot-Savart | Finite element |
| Magnetic field | Zinkiewicz formulation |
| Rod element | Wikswo equation |
| Plate element | Current distributions |

20. ABSTRACT (Continue on reverse side if necessary and identify by block number)

Biot-Savart law magnetic field integration equations are derived for rod and plate elements, and for volume interface regions from an equation due to Wikswo. These equations have applications for problems where current distributions are present over extended volumes and are calculated on the basis of a finite element electric field analysis. The Biot-Savart field so calculated can be used in a further finite element analysis of the magnetic field about a body of high permeability located in the same region as the electric field.

DD FORM 1473 1 JAN 73 EDITION OF 1 NOV 65 IS OBSOLETE
S/N 0102-014-6601

405918

# TABLE OF CONTENTS

## LIST OF ILLUSTRATIONS

# CALCULATION OF THE BIOT-SAVART LAW MAGNETIC FIELD USING CURRENT DISTRIBUTIONS OBTAINED FROM A FINITE ELEMENT ANALYSIS

## INTRODUCTION

Three-dimensional static magnetic field solutions using finite elements have been formulated using both scalar and vector potential functions. Guancial and DasGupta,[1] Frye and Kasper,[2] and Zienkiewicz[3] have addressed the vector potential formulation.

The use of scalar potential functions provides great computational advantages over vector potential functions, since the number of unknowns at a grid point is reduced from three to one. Zienkiewicz et al.[4] showed that a finite element scalar formulation was possible using the Biot-Savart law to account for current terms. Armstrong et al.[5] indicated how the Zienkiewicz formulation could be improved to eliminate ill-formed matrices by a breakup of the problem region into domains using different scalar potentials

Although the use of the scalar potential function gives great economy in the solution of the finite element equations, there are problems where the evaluation of the Biot-Savart magnetic field requires much computation. Typically such problems arise where an object produces electric currents internally in its own structure and externally in the infinite conducting medium in which it is embedded. Figure 1 shows a diagram of such a problem. Wikswo[6] shows how the evaluation of the Biot-Savart law magnetic field for such a problem can be reduced to an integration over boundaries where there is a change in media conductivity and over regions where current sources are present. Often, when the magnetic field around such an object must be evaluated, the currents due to the electric field are calculated using finite element techniques. This is particularly true if the object is of complex shape or has unusual electric field boundary conditions with the infinite medium. Typically, the finite element electric field model of an object will be made up of rod and plate elements, although volume elements may sometimes also be necessary. The infinite medium is modeled as a set of volume elements with an appropriate boundary condition to terminate the finite element mesh. The purpose of this report is to show the derivation of equations from Wikswo's formulation for evaluating the Biot-Savart law magnetic field by using currents obtained from a finite element electric field analysis.

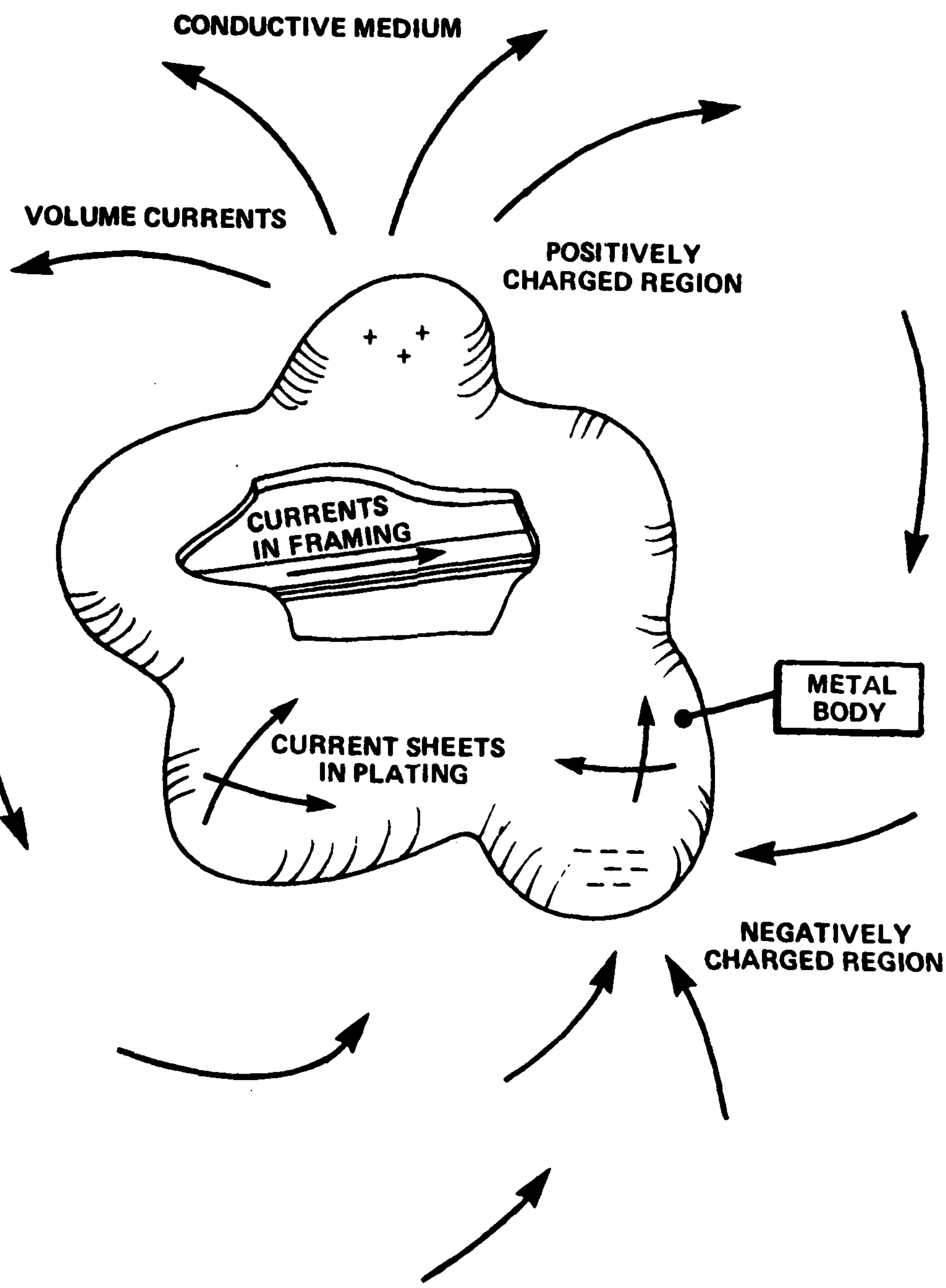


Figure 1. Problem of Internal and External Currents

# THEORETICAL BACKGROUND

In the scalar potential finite element formulations for static magnetic fields,[4] the total field is assumed to be equal to the sum of two components.

$$\vec{H} = \vec{H}_c + \vec{H}_m \ . \tag{1}$$

Component $\vec{H}_c$ is the Biot-Savart law magnetic field strength, and component $\vec{H}_m$ is the gradient of a scalar potential function.

$$\vec{H}_c(\vec{R}) = \frac{1}{4\pi} \int_{V'} \frac{\vec{J} \times (\vec{R}-\vec{R}')}{|\vec{R}-\vec{R}'|^3} \, dV' \tag{2}$$

$$\vec{H}_m = \vec{\nabla}\phi \ , \tag{3}$$

where $\vec{J}$ is some known current density distribution; $\vec{R}$ is the position vector to the point where $\vec{H}_c$ is to be evaluated, $\vec{R}'$ is the position vector of dV', the element volume of the conductor with current $\vec{J}$; and $\phi$ is the unknown scalar potential function.

Use of this assumed solution for the magnetic field strength automatically satisfies the field relation between magnetic field strength and current density:

$$\vec{\nabla} \times \vec{H} = \vec{\nabla} \times \vec{H}_c = \vec{J} \tag{4}$$

since $$\vec{\nabla} \times \vec{H}_m = \vec{\nabla} \times \vec{\nabla}\phi = 0 \ . \tag{5}$$

The remaining field relation requiring that the divergence of the flux density be zero establishes the required relation for determining the scalar potential function:

$$\vec{\nabla} \cdot \vec{B} = 0 \tag{6}$$

$$\vec{\nabla} \cdot \mu(\vec{\nabla}\phi) = -\vec{\nabla} \cdot \mu\vec{H}_c \ . \tag{7}$$

The finite element formulation given by Zienkiewicz et al.[4] for the solution of the field equation results in a matrix equation that relates a set of discrete scalar potential unknowns {$\phi$} to a set of loadings {f} obtained from the Biot-Savart law magnetic field strengths via a matrix [K] calculated with finite element interpolation functions $N_i$.

$$[K]\{\phi\} = \{f\} \tag{8}$$

$$K_{ij} = \int_V (\vec{\nabla}N_i) \cdot \mu(\vec{\nabla}N_j) \, dV \tag{9}$$

$$f_i = -\int_V (\vec{\nabla} N_i) \cdot \mu \vec{H}_c \, dV . \tag{10}$$

It is not necessary to discuss details of the finite element technique since all such details are standard and are discussed fully elsewhere.[7]

The solution of the field problem proceeds by, first, constructing an appropriate finite element model; second, calculating the Biot-Savart magnetic field strengths from the known current distributions; third, computing the loadings $f_i$ from equation (10); fourth, solving the matrix equation (8) for $\{\phi\}$; and finally, fifth, adding the potential gradients obtained from the finite element solution to the Biot-Savart field strength to obtain the total field result. The finite element solution acts as a correction to the Biot-Savart law field strength to account for magnetization existing in materials with permeability other than that of free space.

For problems with infinite conductor domains, the evaluation of the Biot-Savart law magnetic field value from equation (2) requires a great amount of computation because the diffuse nature of the current densities results in an extensive required region of integration. Wikswo[6] has shown, in the case where current densities are known to approach zero in regions of the infinite conducting medium removed from the domain of interest, that equation (2) can be replaced by the following relation:

$$\vec{H}_c(\vec{R}) = \frac{1}{4\pi} \int_{V'} \frac{\vec{\nabla}' \times \vec{J}(\vec{R}')}{|\vec{R} - \vec{R}'|} \, dV' . \tag{11}$$

The advantage to this relation is that, since steady currents can be related to the gradient of a scalar potential function, the curl of the current density is zero at all points in the volume of the problem except at surfaces where there is a change in conductivity or a current source. Thus, the integration of equation (11) reduces from a volume integration to a surface integration. For practical purposes we can break this surface integration into that over the surface of rods, plates, and volume conductivity interfaces. Most metal structures can be characterized, for the purpose of defining current distributions, as a collection of rods that carry currents in a one-dimensional manner and of plates with two-dimensional current sheets. The currents in the conductive medium in which the metal body is embedded can be accounted for by integrating over the interface between the surface of the metal body and the conductive medium, and along the interfaces of differing conductivity in the media. In the following sections, separate equations will be developed from equation (11) for the rod and plate surfaces and the volume interface surfaces. The equations are developed based on the assumption that the current density outside the region of the rod, plate, or volume is zero.

It will later be shown that the summation of separate integrations appropriately accounts for the situations where this assumption is not the case.

## INTEGRATION FOR RODS

Figure 2 shows the rod geometry and the coordinate systems used to describe the rod integrations. The rod axis is assumed to lie along a line between two points in space called grid points 1 and 2. The two grid points have their position in space defined by global coordinates x, y, and z. The rod axial coordinate $\hat{z}_R$ is taken as having its origin at grid point 1 and as having a positive sign in the direction of grid point 2. The axial coordinate direction vector is given by $z_R$.

$$\hat{z}_R = \hat{x}\,\frac{(x_2 - x_1)}{|\vec{R}_2 - \vec{R}_1|} + \hat{y}\,\frac{(y_2 - y_1)}{|\vec{R}_2 - \vec{R}_1|} + \hat{z}\,\frac{(z_2 - z_1)}{|\vec{R}_2 - \vec{R}_1|} \;. \tag{12}$$

The rod coordinate direction vector $\hat{x}_R$ is taken as the cross product of the global $\hat{y}$ direction and the $\hat{z}_R$ direction:

$$\hat{x}_R = \frac{\hat{y} \times \hat{z}_R}{|\hat{y} \times \hat{z}_R|} \;. \tag{13}$$

In the case where $\hat{y}$ and $\hat{z}_R$ are parallel, $\hat{x}_R$ is taken as being the same as $\hat{x}$. The rod coordinate direction vector $\hat{y}_R$ is the cross product of the $\hat{z}_R$ direction and the $\hat{x}_R$ direction:

$$\hat{y}_R = \hat{z}_R \times \hat{x}_R \;. \tag{14}$$

The $\hat{x}_R$ and $\hat{y}_R$ direction vectors can be expressed in terms of their respective components as

$$\hat{x}_R = \hat{x}\,X_{Rx} + \hat{y}\,X_{Ry} + \hat{z}\,X_{Rz} \tag{15}$$

$$\hat{y}_R = \hat{x}\,Y_{Rx} + \hat{y}\,Y_{Ry} + \hat{z}\,Y_{Rz} \;. \tag{16}$$

The rod is assumed to have a circular cross section and to have a radius (a) that is small with respect to the distance to the point where the Biot-Savart law magnetic field value is to be calculated. In other words, the calculations are not to be made in the nearfield of the rod, at least from the standpoint of rod cross-sectional geometry.

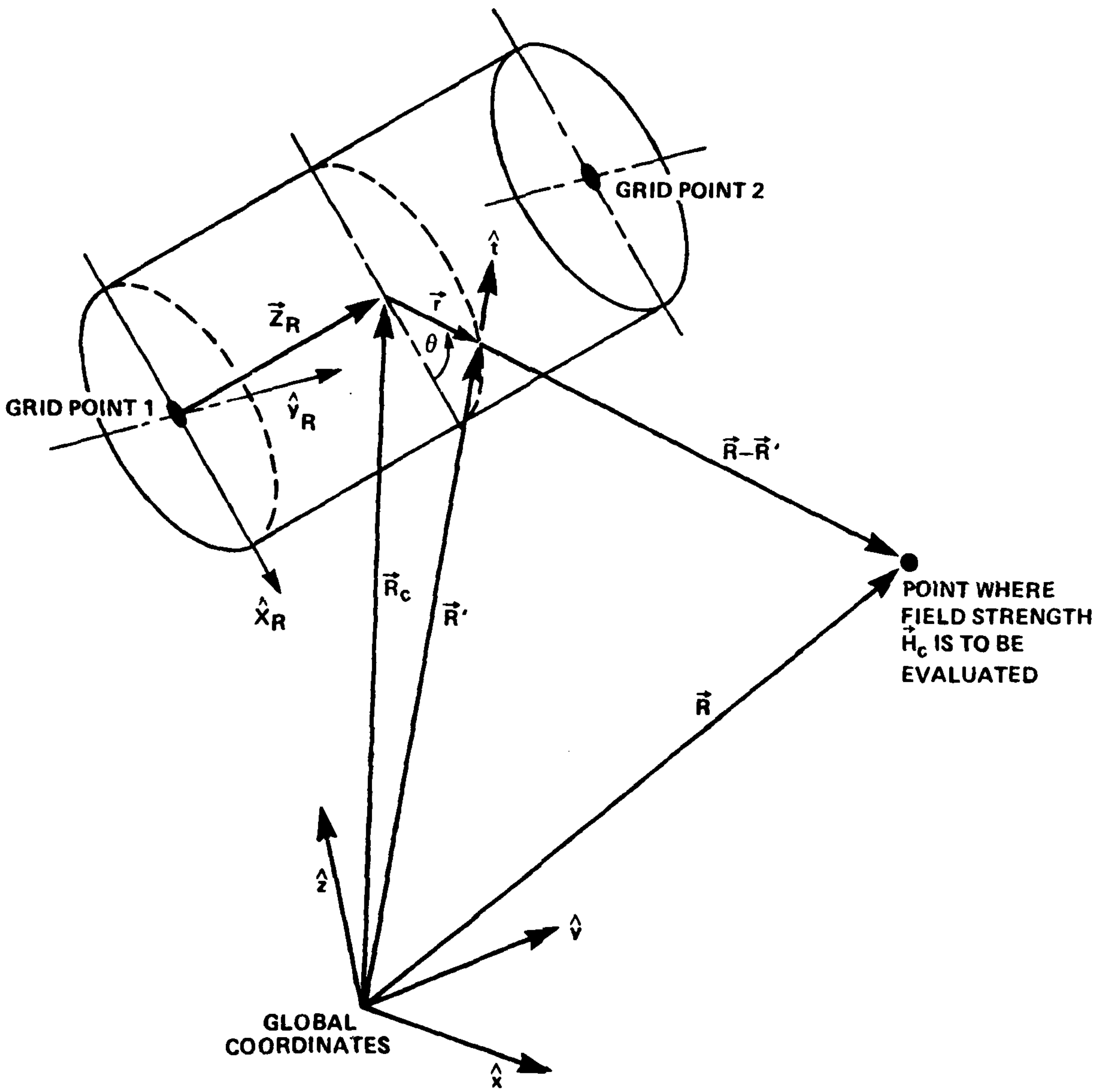


Figure 2. Rod Geometry and Coordinate Systems

$$a \ll |\vec{R} - \vec{R}'| \tag{17}$$

Using cylindrical coordinates, we can define the radial rod direction $\hat{r}$ and tangential direction $\hat{t}$ in terms of the $\hat{x}_R$ and $\hat{y}_R$ directions as

$$\hat{r} = \cos\theta\ \hat{x}_R + \sin\theta\ \hat{y}_R \tag{18}$$

$$\hat{t} = -\sin\theta\ \hat{x}_R + \cos\theta\ \hat{y}_R\ . \tag{19}$$

The vector $\vec{R} - \vec{R}'$ can be rewritten as

$$\vec{R} - \vec{R}' = [\vec{R} - (\vec{R}_c + \vec{r})]\ , \tag{20}$$

where
$$\vec{R}_c = \hat{x}\ (x_1 + \vec{z}_R\cdot\hat{x}) + \hat{y}\ (y_1 + \vec{z}_R\cdot\hat{y}) + \hat{z}\ (z_1 + \vec{z}_R\cdot\hat{z}) \tag{21}$$

$$\vec{z}_R = \hat{z}_R\ z_R \tag{22}$$

$$\vec{r} = \hat{r}\ r\ . \tag{23}$$

$z_R$ and r are the amplitudes of the axial and radial coordinates. $\vec{R}_c$ is the vector to a point on the rod axis. $\vec{R}_c$ can also be written in terms of its global coordinates as

$$\vec{R}_c = x_c\hat{x} + y_c\hat{y} + z_c\hat{z}\ . \tag{24}$$

Substituting equations (15), (16), (18), (19), and (24) into equation (20) and evaluating the absolute value of the vector expression gives the following result for $|\vec{R} - \vec{R}'|$:

$$\begin{aligned}|\vec{R} - \vec{R}'| = \Big\{&(x - x_c - r\ [\cos\theta X_{Rx} + \sin\theta Y_{Rx}])^2 \\ &+ (y - y_c - r\ [\cos\theta X_{Ry} + \sin\theta Y_{Ry}])^2 \\ &+ (z - z_c - r\ [\cos\theta X_{Rz} + \sin\theta Y_{Rz}])^2\Big\}^{1/2}\ .\end{aligned} \tag{25}$$

Since r will always be small in relation to $|\vec{R} - \vec{R}_c|$, $|\vec{R} - \vec{R}'|$ can be accurately approximated as

$$\begin{aligned}|\vec{R} - \vec{R}'| = \frac{1}{|\vec{R} - \vec{R}_c|}\Big(&|\vec{R} - \vec{R}_c|^2 - r(x-x_c)\ [\cos\theta X_{Rx} + \sin\theta Y_{Rx}] \\ &- r(y-y_c)\ [\cos\theta X_{Ry} + \sin\theta Y_{Ry}] \\ &- r(z-z_c)\ [\cos\theta X_{Rz} + \sin\theta Y_{Rz}]\Big)\ .\end{aligned} \tag{26}$$

The current in the rod is assumed to be flowing in the axial direction of the rod; thus, $J_{Rx}$ and $J_{Ry}$ components of the $\vec{J}$ current density are zero. The curl of $\vec{J}$ in terms of rod coordinates is given by

$$\vec{\nabla}' \times \vec{J} = \begin{vmatrix} \hat{r} & \hat{t} & \hat{z}_R \\ \frac{\partial}{\partial r} & \frac{\partial}{\partial t} & \frac{\partial}{\partial z_R} \\ 0 & 0 & J_{Rz} \end{vmatrix} = \hat{r}\left[\frac{\partial J_{Rz}}{\partial t}\right] + \hat{t}\left[-\frac{\partial J_{Rz}}{\partial r}\right] + z_r\,(0) . \quad (27)$$

If the rod current density is assumed constant over the rod, then $\frac{\partial J_{Rz}}{\partial t}$ is always zero, even along the sides of the rod parallel to the axis. Thus, the curl of $\vec{J}$ simplifies to

$$\vec{\nabla}' \times \vec{J} = -\hat{t}\,\frac{\partial J_{Rz}}{\partial r} . \quad (28)$$

The derivative $\frac{\partial J_{Rz}}{\partial r}$ is zero at all points on the rod except along the rod longitudinal surface, where the value of $J_{Rz}$ is assumed to drop to a zero value.

In evaluating the integral of equation (11) it is necessary to evaluate only the limit over a film of volume at the rod longitudinal surface as the film thickness goes to zero. Figure 3 illustrates such a film of volume. The differential volume dV' can be expressed as

$$dV' = a\,\delta r\,d\theta\,dz_R . \quad (29)$$

The partial derivative $\frac{\partial J_{Rz}}{\partial r}$ can also be expressed as the following limit:

$$\frac{\partial J_{Rz}}{\partial r} = \lim_{\delta r \to o} \frac{J_{Rz}(a + \frac{\delta r}{2}) - J_{Rz}(a - \frac{\delta r}{2})}{\delta r} . \quad (30)$$

The combination of the terms of equations (29) and (30) produces the following expression:

$$\left.\frac{\partial J_{Rz}}{\partial r}\,dV'\right|_{r \to a} = \lim_{\delta r \to o} \frac{J_{Rz}(a + \frac{\delta r}{2}) - J_{Rz}(a - \frac{\delta r}{2})}{\delta r}\,a\,\delta r\,d\theta\,dz_R . \quad (31)$$

$J_{Rz}\,(a + \frac{\delta r}{2})$ is interpreted to be the current density just outside the rod volume and is zero. The current density $J_{Rz}\,(a - \frac{\delta r}{2})$ is the

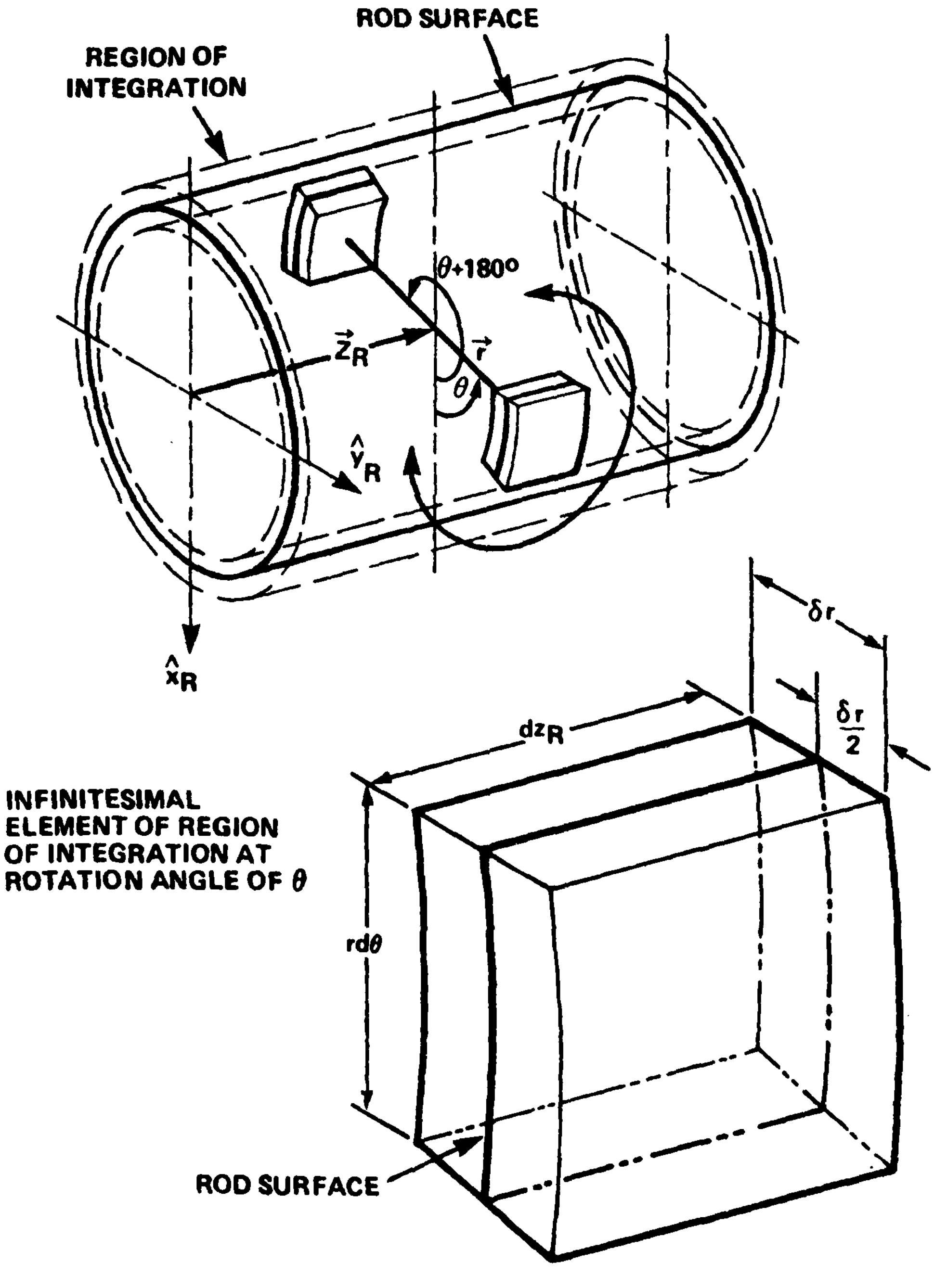


Figure 3. Evaluating the Limit of a Film of Volume

current density just inside the rod surface and is equal to $J_{Rz}$. Thus, expression (31) becomes, after the evaluation of the limit,

$$\left.\frac{\partial J_{Rz}}{\partial r}\, dV'\right|_{r\to a} = -J_{Rz} a d\theta dz_R \, . \tag{32}$$

The volume integration for the rod given by equation (11) then reduces to the following integration over the rod's longitudinal surface:

$$\vec{H}_c\,(\vec{R}) = \frac{1}{4\pi}\int_0^L\int_0^{2\pi} \frac{\hat{t}\; J_{Rz}}{|R-R'|}\, a d\theta dz_R \, . \tag{33}$$

The integration limit from 0 to $2\pi$ can be changed to a limit that varies from 0 to $\pi$ by adding up the contributions of elemental surface areas at $\theta$ and $\theta + \pi$ radians simultaneously:

$$\vec{H}_c\,(\vec{R}) = \frac{1}{4\pi}\int_0^L\int_0^{\pi} \left[\frac{\hat{t}\; J_{Rz}}{|R-R'|_\theta} - \frac{\hat{t}\; J_{Rz}}{|R-R'|_{\theta+\pi}}\right] a d\theta dz_r \, . \tag{34}$$

The first term in the integration accounts for the elemental area at $\theta$, and the second term accounts for the elemental term at $\theta + \pi$. Here we have accounted with a minus sign for the fact that the tangent vector at $\theta + \pi$ is in the opposite direction from the tangent vector at $\theta$. The terms $|\vec{R}-\vec{R}'|_\theta$ and $|\vec{R}-\vec{R}'|_{\theta+\pi}$ can be calculated from equation (26) by setting $r = a$:

$$|\vec{R}-\vec{R}|_\theta = \frac{1}{|\vec{R}-\vec{R}_c|}\left[|\vec{R}-\vec{R}_c|^2 - a(\vec{R}-\vec{R}_c)\cdot\hat{r}\right] \tag{35}$$

$$|\vec{R}-\vec{R}|_{\theta+\pi} = \frac{1}{|\vec{R}-\vec{R}_c|}\left[|\vec{R}-\vec{R}_c|^2 + a(\vec{R}-\vec{R}_c)\cdot\hat{r}\right] \, . \tag{36}$$

If equations (35) and (36) are substituted into equation (34) and the expression inside the integration is placed under a common denominator, we obtain the following:

$$\vec{H}_c\,(\vec{R}) = \frac{1}{4\pi}\int_0^L\int_0^{\pi} \frac{-2\hat{t}\; J_{Rz}\; a^2(\vec{R}-\vec{R}_c)\cdot\hat{r}}{|\vec{R}-\vec{R}_c|^3}\, d\theta dz_R \, . \tag{37}$$

Performance of the integration with respect to $\theta$, which involves the algebraic expansion of equation (37), results in

$$\vec{H}_c(\vec{R}) = \frac{1}{4\pi} \int_0^L \frac{-\pi a^2 \, J_{Rz}(\vec{R}-\vec{R}_c) \times \hat{r}_R \times \hat{y}_R}{|\vec{R}-\vec{R}_c|^3} dz_R \ . \tag{38}$$

If $I_R$ is the total current flowing in the rod, then $J_{Rz}$ is equal to $I_R$ divided by the rod cross-sectional area:

$$J_{Rz} = \frac{I_R}{\pi a^2} \ . \tag{39}$$

Also $$\hat{z}_R = \hat{x}_R \times \hat{y}_R \tag{40}$$

Substitution of equations (39) and (40) into equation (38) results in the final form for the integration of the rod current contribution to the Biot-Savart law magnetic field strength:

$$\vec{H}_c(\vec{R}) = \frac{1}{4\pi} \int_0^L \frac{I_R \hat{z}_R \times (\vec{R}-\vec{R}_c)}{|\vec{R}-\vec{R}_c|^3} dz_R \ . \tag{41}$$

The integration with respect to a volume given by equation (11) is then reduced for the rod to an integration along the rod axis.

## INTEGRATION FOR PLATES

Figure 4 shows the coordinate systems used in the development of expressions for integrating over the region of plates. The plate shown in the figure is quadrilateral, but the coordinate system definition is essentially the same for triangular plates. The plate is defined by four grid points, at the vertices of the plate edges, that have their locations specified in terms of global $\hat{x}$, $\hat{y}$, and $\hat{z}$ coordinate directions. These points are known as grid points 1, 2, 3, and 4. The normal to the plate surface can be calculated by taking the cross product of a vector directed between the first and second grid points and a vector directed between the first and fourth grid points and normalizing the result:

$$\hat{n} = \frac{\vec{\alpha} \times \vec{\beta}}{|\vec{\alpha} \times \vec{\beta}|} \ , \tag{42}$$

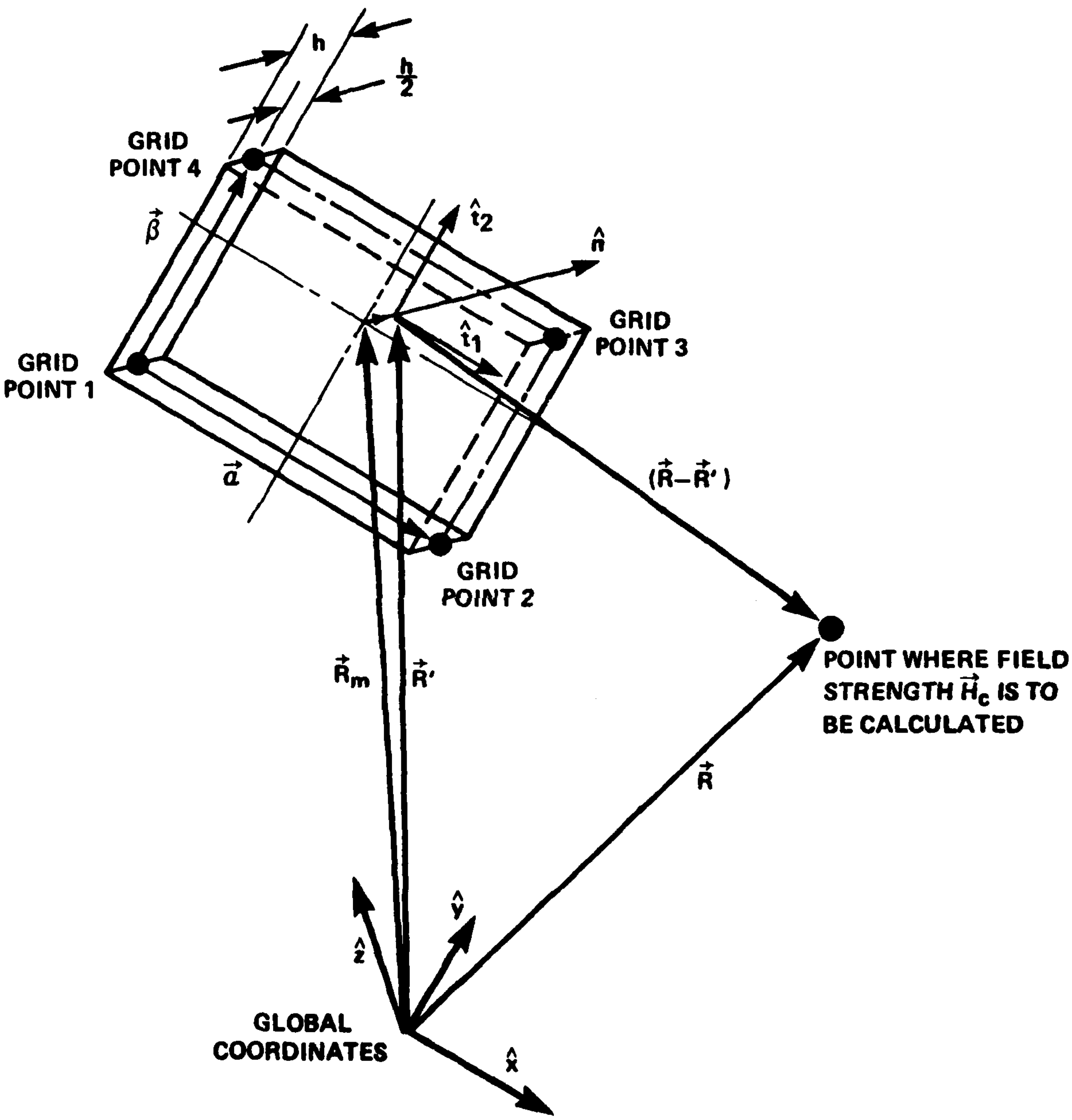


Figure 4. Coordinate Systems for Integrating Over the Region of Plates

where $$\vec{\alpha} = (x_2 - x_1)\,\hat{x} + (y_2 - y_1)\,\hat{y} + (z_2 - z_1)\,\hat{z} \tag{43}$$

$$\vec{\beta} = (x_4 - x_1)\,\hat{x} + (y_4 - y_1)\,\hat{y} + (z_4 - z_1)\,\hat{z} \quad . \tag{44}$$

$x_1$, $y_1$, $z_1$, $x_2$, $y_2$, $z_2$, and $x_4$, $y_4$, $z_4$, are global coordinates of the first, second, and fourth grid points,respectively.

The first tangential plate coordinate direction,known as $\hat{t}_1$,is in the same direction as $\alpha$;

$$\hat{t}_1 = \frac{\vec{\alpha}}{|\alpha|} \quad . \tag{45}$$

The second tangential coordinate direction is obtained by taking the cross product of $\hat{n}$ and $\hat{t}_1$:

$$\hat{t}_2 = \hat{n} \times \hat{t}_1 \quad . \tag{46}$$

The advantage of using these coordinate directions is that finite element programs that analyze current fields often use these coordinates when listing components of a current vector.

The curl of the current density for a current flowing in the plate is

$$\vec{\nabla}' \times \vec{J} = \hat{n}\left(\frac{\partial J_{t_2}}{\partial t_1} - \frac{\partial J_{t_1}}{\partial t_2}\right) - \hat{t}_1\left(\frac{\partial J_{t_2}}{\partial n}\right) + \hat{t}_2\left(\frac{\partial J_{t_1}}{\partial n}\right) \quad . \tag{47}$$

Note that there is no component of current density normal to the plate as all currents are assumed to be flowing parallel to the plane of the plate.

The current in the plate can be expressed as being equal to the plate material conductivity times the gradient of a potential function:

$$J_{t_1} = \sigma \frac{\partial \phi}{\partial t_1} \tag{48}$$

$$J_{t_2} = \sigma \frac{\partial \phi}{\partial t_2} \quad . \tag{49}$$

Substituting equations (48) and (49) into the first term of equation (47), we have

$$\frac{\partial J_{t_2}}{\partial t_1} - \frac{\partial J_{t_1}}{\partial t_2} = \frac{\partial^2 \phi}{\partial t_1 \partial t_2} - \frac{\partial^2 \phi}{\partial t_1 \partial t_2} = 0 \quad . \tag{50}$$

The component of the curl term normal to the plate drops out. The remaining terms in the curl relation are normal derivatives of current terms tangent to the plane of the plate. These terms are zero everywhere except at the surface since the current is assumed not to vary across the plate thickness. At the surface, the current vector amplitude changes abruptly from some value to zero. Figure 5 shows a diagram of the elemental volumes at the upper and lower surfaces of the plate. The expression for the elemental volume may be written as

$$dV = \delta T \, dt_1 \, dt_2 . \tag{51}$$

The derivatives $\frac{\partial J_{t_1}}{\partial n}$ and $\frac{\partial J_{t_2}}{\partial n}$ can also be written as limits

$$\frac{\partial J_{t_1}}{\partial n} = \lim_{\delta T \to o} \left[ \frac{J_{t_1}\left(\frac{h}{2} + \frac{\delta T}{2}\right) - J_{t_1}\left(\frac{h}{2} - \frac{\delta T}{2}\right)}{\delta T} \right] \tag{52}$$

$$\frac{\partial J_{t_2}}{\partial n} = \lim_{\delta T \to o} \left[ \frac{J_{t_2}\left(\frac{h}{2} + \frac{\delta T}{2}\right) - J_{t_1}\left(\frac{h}{2} - \frac{\delta T}{2}\right)}{\delta T} \right] . \tag{53}$$

On the upper plate surface the current densities above the plate are zero, and on the lower surface the current densities below the plate are zero:

$$\text{UPPER SURFACE} \quad J_{t_1}\left(\frac{h}{2} + \frac{\delta T}{2}\right) = J_{t_2}\left(\frac{h}{2} + \frac{\delta T}{2}\right) = 0 \tag{54}$$

$$\text{LOWER SURFACE} \quad J_{t_1}\left(\frac{h}{2} - \frac{\delta T}{2}\right) = J_{t_2}\left(\frac{h}{2} - \frac{\delta T}{2}\right) = 0 . \tag{55}$$

On the upper surface the current densities below the surface are the plate current densities, and on the lower surface the current densities above the surface are the plate densities:

$$\text{UPPER SURFACE} \begin{cases} J_{t_1}\left(\frac{h}{2} - \frac{\delta T}{2}\right) = J_{t_1} & (56) \\ J_{t_2}\left(\frac{h}{2} - \frac{\delta T}{2}\right) = J_{t_2} & (57) \end{cases}$$

$$\text{LOWER SURFACE} \begin{cases} J_{t_1}\left(\frac{h}{2} + \frac{\delta T}{2}\right) = J_{t_1} & (58) \\ J_{t_2}\left(\frac{h}{2} + \frac{\delta T}{2}\right) = J_{t_2} . & (59) \end{cases}$$

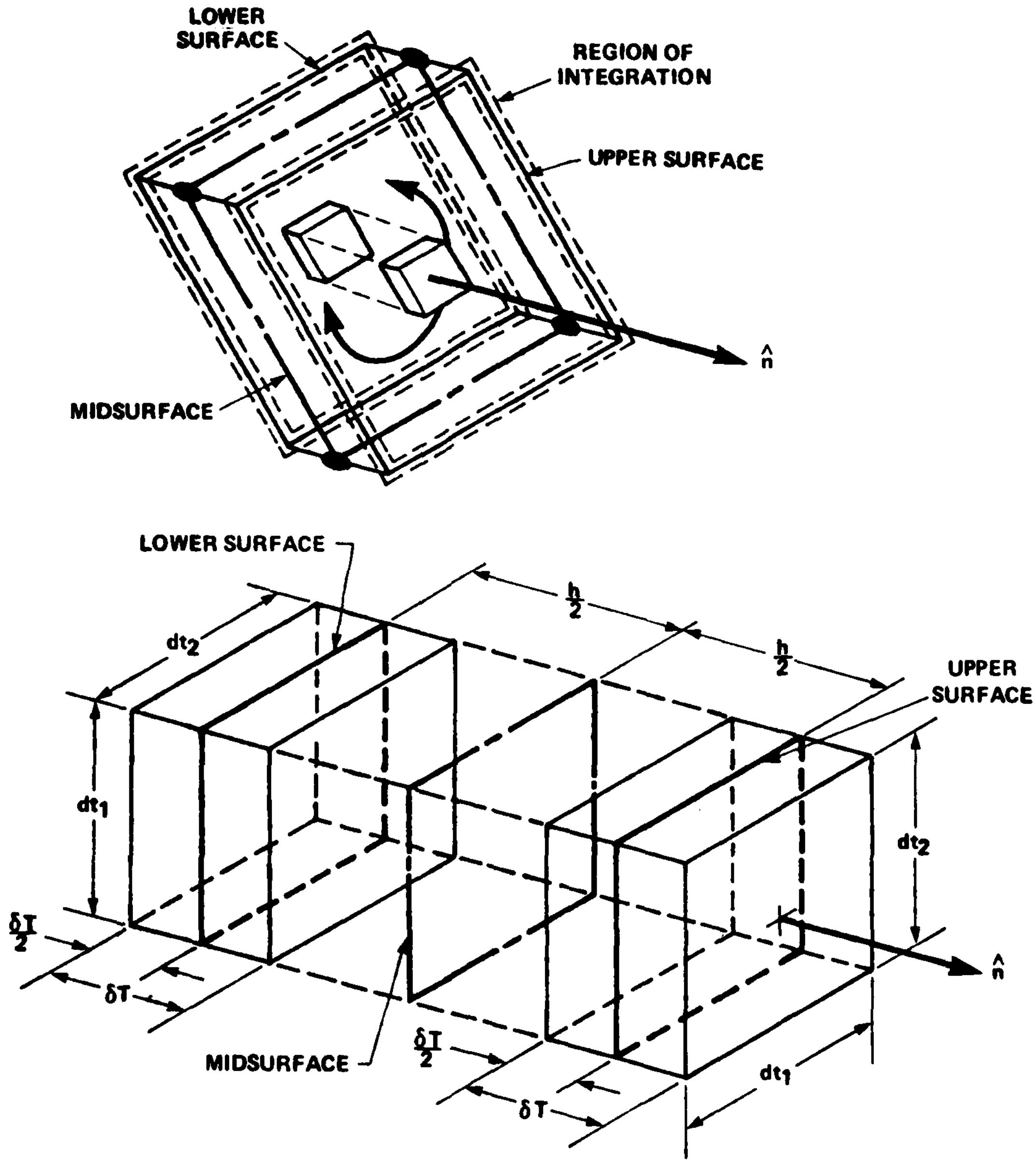


Figure 5. Elemental Volumes at Upper and Lower Surfaces of Plate

Substituting equation (47) and equations (51) through (59) into equation (11) gives

$$\vec{H}_c(\vec{R}) = \frac{1}{4\pi}\int\left\{\left(\frac{\hat{t}_1 J_{t_2} - \hat{t}_2 J_{t_1}}{|\vec{R} - \vec{R}'|_{us}}\right) - \left(\frac{\hat{t}_1 J_{t_2} - \hat{t}_2 J_{t_1}}{|\vec{R} - \vec{R}'|_{ls}}\right)\right\} dt_1\, dt_2 \,, \quad (60)$$

where $|\vec{R} - \vec{R}'|_{us}$ is the amplitude of the vector to the upper surface

and $|\vec{R} - \vec{R}'|_{ls}$ is the amplitude of the vector to the lower surface .

The amplitudes $|\vec{R} - \vec{R}'|_{us}$ and $|\vec{R} - \vec{R}'|_{ls}$ can be written in terms of vectors to the plate midsurface and the normal of the plate:

$$|\vec{R} - \vec{R}'|_{us} = |\vec{R} - \vec{R}_m - \frac{h}{2}\hat{n}| \quad (61)$$

$$|\vec{R} - \vec{R}'|_{ls} = |\vec{R} - \vec{R}_m + \frac{h}{2}\hat{n}| \,, \quad (62)$$

where $\vec{R}_m$ is the vector to the midsurface.

Under the assumption that the plate thickness is small in relation to the distance to the point where the field strength is to be calculated, equations (61) and (62) can be approximated by

$$|\vec{R} - \vec{R}'|_{us} \approx \frac{1}{|\vec{R} - \vec{R}_m|}\left[|\vec{R} - \vec{R}_m|^2 - \frac{h}{2}n\cdot(\vec{R} - \vec{R}_m)\right] \quad (63)$$

$$|\vec{R} - \vec{R}'|_{ls} \approx \frac{1}{|\vec{R} - \vec{R}_m|}\left[|\vec{R} - \vec{R}_m|^2 + \frac{h}{2}n\cdot(\vec{R} - \vec{R}_m)\right] \,. \quad (64)$$

Substituting equations (63) and (64) into equation (60) and placing the two terms in the integral under a common denominator results in

$$\vec{H}_c(\vec{R}) = \frac{1}{4\pi}\int_{S_m} \frac{h\left[\hat{n}\cdot(\vec{R} - \vec{R}_m)(\vec{J} \times \hat{n})\right]}{|\vec{R} - \vec{R}_m|^3}\, dt_1\, dt_2 \,. \quad (65)$$

If the sheet current $\vec{I}_s$ is defined as the current density times the thickness of the plate, then equation (65) can be rewritten in the following way:

$$\vec{H}_c(\vec{R}) = \frac{1}{4\pi}\int_{S_m} \frac{\left[\hat{n}\cdot(\vec{R} - \vec{R}_m)(\vec{I}_s \times \hat{n})\right]}{|\vec{R} - \vec{R}_m|^3}\, dt_1\, dt_2 \,. \quad (66)$$

Thus,the integration of the plate is reduced to an integral over the midsurface of the plate.

## VOLUME INTERSECTION SURFACE

Figure 6 shows the coordinate systems used in the development of expressions for integrating over surface regions of volumes. The region shown in the figure is quadrilateral, but the coordinate system definition is the same for triangular regions. The surface region is defined by four grid points, at the vertices of the region's edges, that have their locations specified in global x, y, and z coordinate directions. The grid points are numbered counterclockwise when viewed from outside the conductive medium. The vector directions n, $t_1$, and $t_2$ are defined in the same manner as with the plate coordinates, i.e., with equations (42), (45), and (46).

In the case of a surface region of a volume, there may be components of current density flowing in a direction normal to the surface as well as tangent to it. Thus, the curl of the current density contains all components of the current density:

$$\vec{\nabla}' \times \vec{J} = \hat{n}\left(\frac{\partial J_{t_2}}{\partial t_1} - \frac{\partial J_{t_1}}{\partial t_2}\right) + \hat{t}\left(\frac{\partial J_n}{\partial t_2} - \frac{\partial J_{t_2}}{\partial n}\right) + \hat{t}_2\left(\frac{\partial J_{t_1}}{\partial n} - \frac{\partial J_n}{\partial t_1}\right) . \quad (67)$$

As with the plate element, the normal component of the curl of $\vec{J}$ always vanishes because the current density can be written as the gradient of a scalar potential function in the region of the conductive medium. In fact, all components of the curl vanish at all points in the domain of the conductive medium except at points on the surface region where the current density vanishes just outside the surface.

Figure 7 shows a diagram of the elemental volume of integration on the surface region of a volume. The expression for the elemental volume may be written as

$$dV = \delta u dt_1 dt_2 . \quad (68)$$

The derivatives $\frac{\partial J_{t_1}}{\partial n}$ and $\frac{\partial J_{t_2}}{\partial n}$ can be written as the following limits:

$$\frac{\partial J_{t_1}}{\partial n} = \lim_{\delta u \to o}\left(\frac{J_{t_1}(\frac{\delta u}{2}) - J_{t_1}(-\frac{\delta u}{2})}{\delta u}\right) \quad (69)$$

$$\frac{\partial J_{t_2}}{\partial n} = \lim_{\delta u \to o}\left(\frac{J_{t_2}(\frac{\delta u}{2}) - J_{t_2}(-\frac{\delta u}{2})}{\delta u}\right) . \quad (70)$$

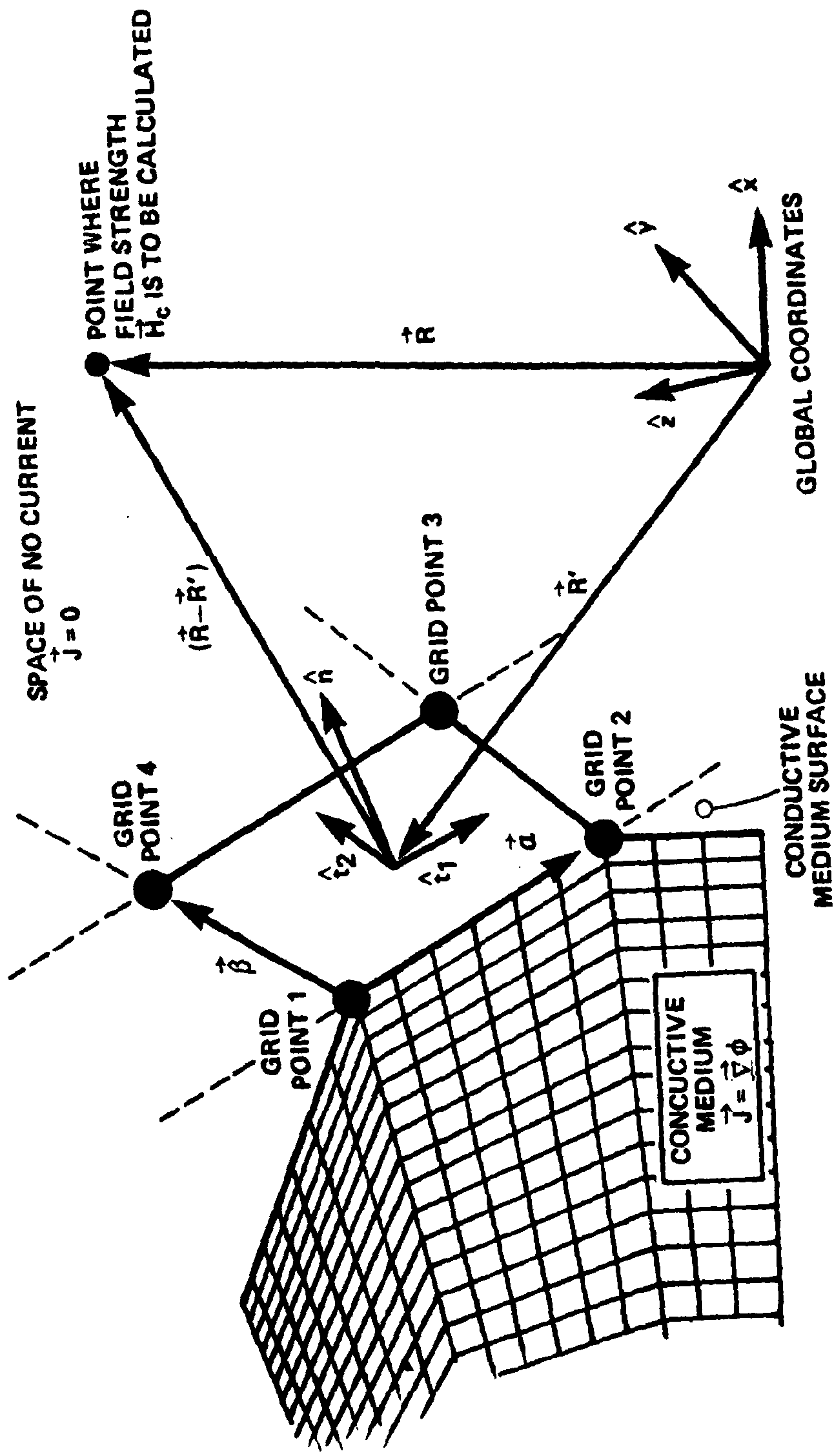


Figure 6. Coordinate Systems for Integrating Over Surface Regions of Volumes

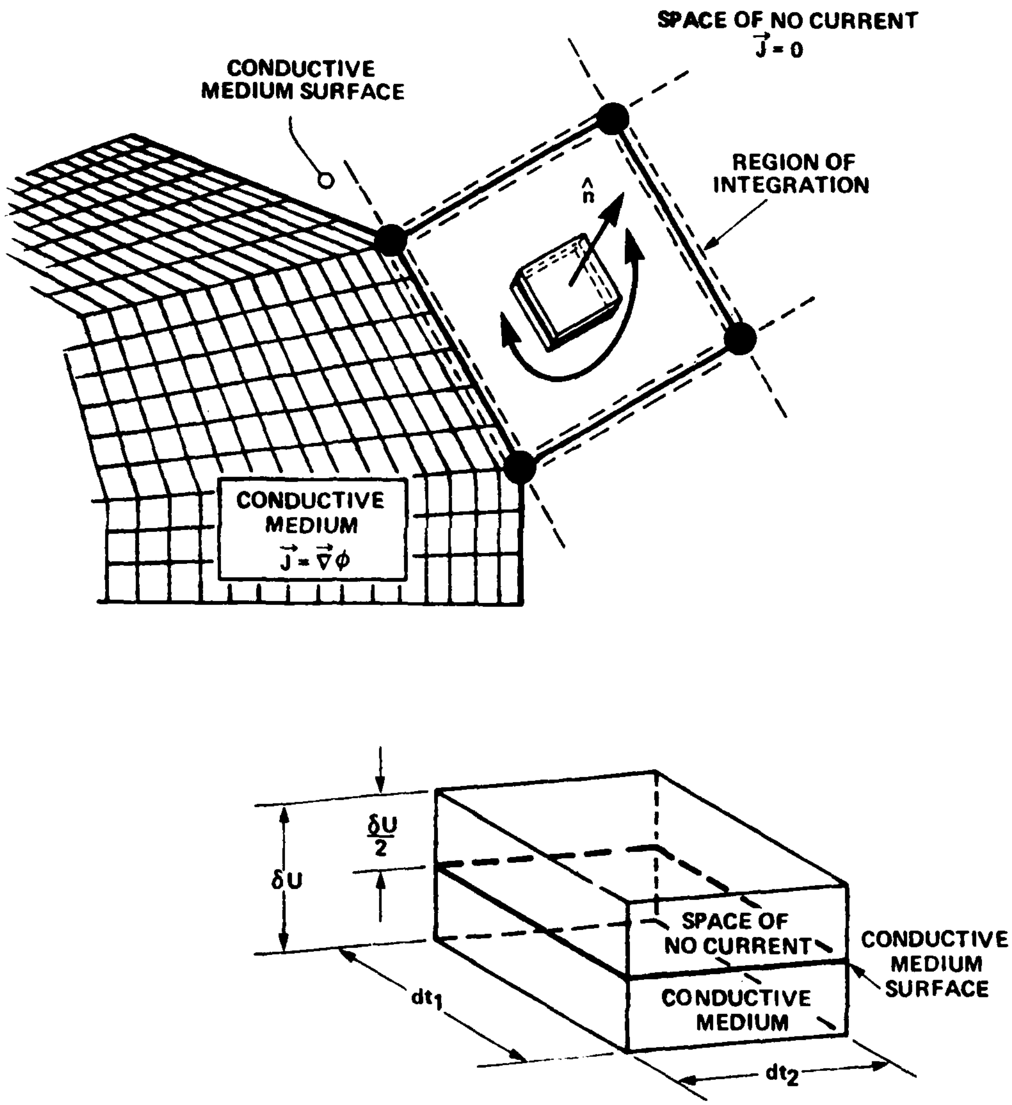


Figure 7. Elemental Volume of Integration on the Surface Region of a Volume

$J_{t_1}(\frac{\delta u}{2})$ and $J_{t_2}(\frac{\delta u}{2})$ refer to current densities just outside the conductive medium and are both zero. $J_{t_1}(-\frac{\delta u}{2})$ and $J_{t_2}(-\frac{\delta u}{2})$ refer to current densities just inside the conductive medium and are equal to $J_{t_1}$ and $J_{t_2}$, respectively.

Using equations (67), (68), (69), and (70) in equation (11) and noting that the curl term in the direction normal to the surface vanishes, we obtain

$$\vec{H}_c(\vec{R}) = \frac{1}{4\pi}\int_S \left\{ \frac{\hat{t}_1 \left[ \lim_{\delta u \to o} \left( \frac{\partial J_n}{\partial t_2} + \frac{J_{t_2}}{\delta u} \right) \delta u \right]}{|\vec{R} - \vec{R}'|} + \frac{\hat{t}_2 \left[ \lim_{\delta u \to o} \left( - \frac{\partial J_n}{\partial t_1} - \frac{J_{t_1}}{\delta u} \right) \delta u \right]}{|\vec{R} - \vec{R}'|} \right\} dt_1 dt_2 \ . \tag{71}$$

Evaluation of the limits of equation (71) results in the final expression for the integration over the surface region. In evaluating the limit it should be noted that the tangential derivatives of the normal component of current are finite since the discontinuity in the normal component of current density, if it exists, is in the direction normal to the surface, not tangential to it:

$$\vec{H}_c(\vec{R}) = \frac{1}{4\pi}\int_S \frac{\vec{J} \times \hat{n}}{|\vec{R} - \vec{R}'|} ds \ . \tag{72}$$

It is interesting that the components of the current density normal to the surface region do not enter into the magnetic field strength calculations. Only tangential current density components are of importance.

## SURFACES WITH NONZERO CURRENT DENSITIES ON BOTH SIDES

In all of the discussions thus far, integration equations have been developed for surfaces that have current densities on one side of the surface and not the other. To consider the case where a current density exists on both sides of a surface, it is necessary only to add the results of two separate integrations where the surface normal is defined separately and with a different positive direction in each integration. Consider figure 8, which shows a surface Γ between two regions, A and B, of differing conductivity. $\vec{J}_A$ is the current density in region A, and $\vec{J}_B$ is the current density in region B.

In the evaluation of the Biot-Savart law magnetic field strength, we have seen that it is necessary to evaluate the integral $\int \frac{\partial J_T}{\partial n}\, dV$ over the surface of the intersection of two regions of differing conductivity. To do this, the limit is taken of the product of the derivative and the infinitesimal volume element as the side of the element approaches zero:

$$\int \frac{\partial J_T}{\partial n}\, dV = \int \lim_{\delta n_B} \frac{J_{T_A} - J_{T_B}}{\delta n_B}\, \delta n_B\, dS \quad . \tag{73}$$

Here we have taken $\delta n_B$ as positive-pointing away from the B region. Equation (73) can easily be rewritten as

$$\int \frac{\partial J_T}{\partial n}\, dV = \int \left\{ \lim_{\delta n_A \to o} \left( \frac{-J_{T_A}}{\delta n_A} \right) + \lim_{\delta n_B \to o} \left( \frac{-J_{T_B}}{\delta n_B} \right) \right\} ds$$

$$= \int \lim_{\delta n_A \to o} \left( \frac{0 - J_{T_A}}{\delta n_A} \right) \delta n_A ds + \int \lim_{\delta n_B \to o} \left( \frac{0 - J_{T_B}}{\delta n_B} \right) \delta n_B ds$$

$$\frac{\partial J_T}{\partial n} = \int \lim_{\delta n_A \to o} \left( \frac{\overbrace{J_{T_A}\left(+\frac{\delta n_A}{2}\right)}^{\textit{taken to be zero}} - J_{T_A}\left(-\frac{\delta n_A}{2}\right)}{\delta n_A} \right) \delta n_A ds$$

$$+ \int \lim_{\delta n_B \to o} \left( \frac{\overbrace{J_{T_B}\left(+\frac{\delta n_B}{2}\right)}^{\textit{taken to be zero}} - J_{T_B}\left(-\frac{\delta n_B}{2}\right)}{\delta n_B} \right) \delta n_A ds$$

$$\frac{\partial J_T}{\partial n} = \underbrace{\int \frac{\partial J_{T_A}}{\partial n_A}\, dV}_{\text{region outside A has zero current density}} + \underbrace{\int \frac{\partial J_{T_B}}{\partial n_B}\, dV}_{\text{region outside B has zero current density}} \tag{74}$$

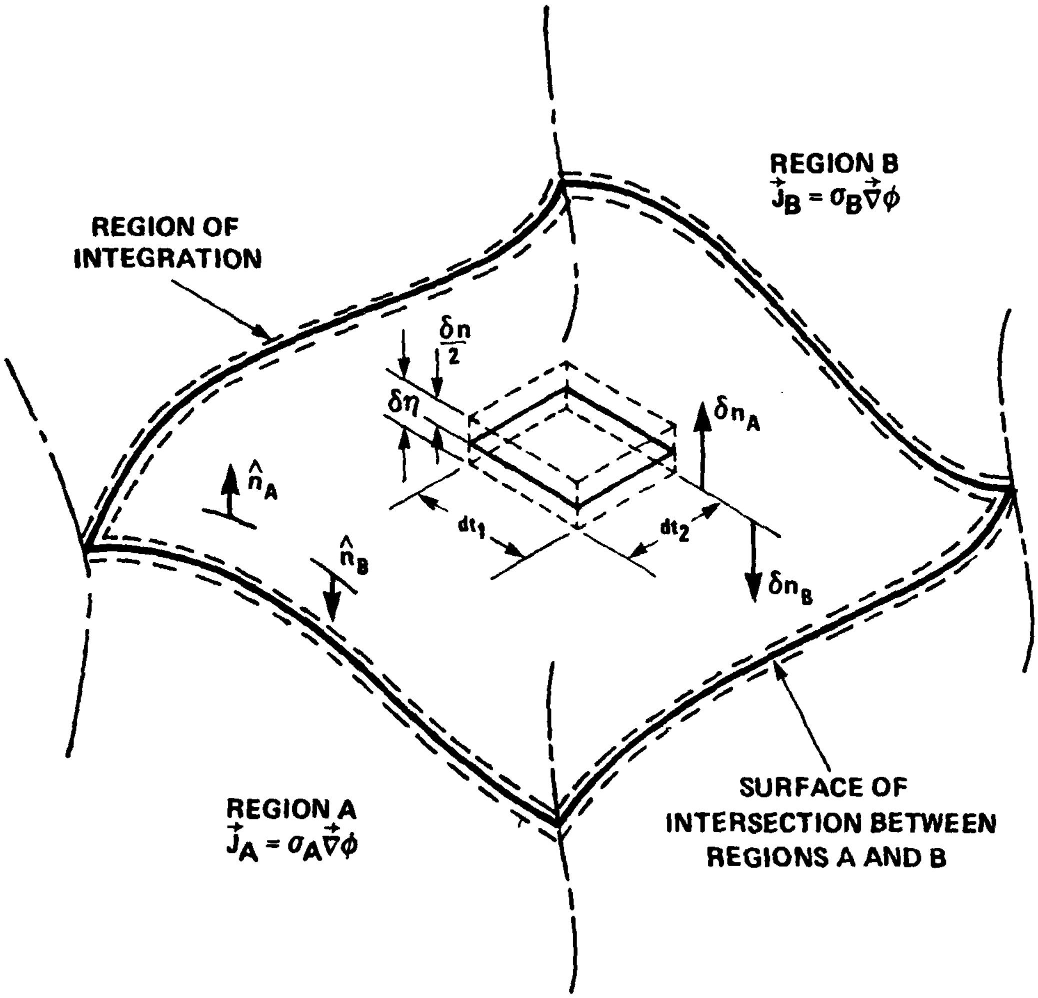


Figure 8. Surface Between Two Regions of Differing Conductivity

The integration over the surface of the intersection between two volumes of differing conductivity is seen to be equivalent to the sum of the separate integrals over the two regions, with the assumption that the current density in all other adjacent regions is zero. As a result, the Biot-Savart law field strength may be evaluated by summing the rod, plate, and volume intersection surface integrations of equations (41), (66), and (72).

This conclusion perhaps could have been reached in a more direct manner by simply noting that equation (11) is the volume integral taken over regions of nonzero current density and that this integration can be evaluated by summing the integration over separate regions.

## REFERENCES


1. E. Guancial and S. DasGupta, "Three-Dimensional Finite Element Program for Magnetic Field Problems," IEEE Transactions on Magnetics, vol. MAG-13, no. 3, May 1977, pp 1012, 1015.

2. J. W. Frye and R. G. Kasper, "Analysis of Magnetic Fields Using Variational Principles and CELAS2 Elements," Sixth NASTRAN Users' Colloquium, NASA Conference Publication 2018, October 4-6, 1977, pp 175, 187.

3. O. C. Zienkiewicz, "The Electromagnetic Problem, Two and Three-Dimensional Treatment by Finite Elements," Dept. Civil Engineering, University College of Swansea, Wales C/R/127/70, 1970.

4. O. C. Zienkiewicz, J. Lyness, and Dr. J. Owen, "Three-Dimensional Magnetic Field Determination Using a Scalar Potential--A Finite Element Solution," IEEE Transactions on Magnetics, vol. MAG-13, no. 5, September 1977, pp 1649, 1656.

5. A. G. Armstrong et al., "The Solution of 3D Magnetostatic Problems Using Scalar Potentials," Rutherford Laboratory Report RL-78-088, Rutherford Laboratory, Chilton, Didcot, Oxon, England OX11 0QZ, September 1978.

6. J. P. Wikswo, "The Calculation of the Magnetic Field from a Current Distribution: Application to Finite Element Techniques," IEEE Transactions on Magnetics, vol. MAG-14, no. 5, September 1978, pp 1076, 1077.

7. O. C. Zienkiewicz, The Finite Element Method in Engineering Science, McGraw-Hill, New York, 1971.

# INITIAL DISTRIBUTION LIST

| Addressee | No. of Copies |
|---|---|
| ONR, Code 427, 483, 412-8, 480, 410, Earth Sciences Division (T. Quinn) | 6 |
| NRL, Code 6451 (J. Davis, W. Meyers, R. Dinger, F. Kelly, D. Forester), Code 6454 (J. Clement) | 6 |
| NAVELECSYSCOMHQ, Code 03, PME-117, -117-21, -117-213, -117-213A, -117-215 | 6 |
| NELC, Code 3300 (R. Moler, H. Hughes, R. Pappert) | 3 |
| DTNSRDC/Annapolis, Code 2704 (W. Andahazy, D. Everstine, F. Baker), Code 2782 (B. Hood, D. Nixon), Code 2813 (E. Bieberich) | 6 |
| DTNSRDC/Cardarock, Code 1548 (R. Knutson), Code 1102.2 (J. Stinson), Code 1844 (M. Hurwitz) | 3 |
| NAVSURFWPNCEN, Code WE-12 (K. Bishop, M. Lackey, W. Menzel, E. Peizer), Code WR-43 (R. Brown, J. Cunningham, Jr., M. Draichman, G. Usher) | 8 |
| NAVCOASTSYSLAB, Code 721 (C. Stewart), Code 773 (K. Allen), Code 792 (M. Wynn, W. Wynn) | 4 |
| NAVSEA, Code 5431 (C. Butler, G. Kahler, D. Muegge) | 3 |
| NAVFACENGSYSCOM, Code FPO-1C (W. Sherwood), Code FPO-1C7 (R. McIntyre, A. Sutherland) | 3 |
| NAVAIR, Code AIR-0632 B (L. Goertzen) | 1 |
| NAVAIRDEVCEN, Code 2022 (J. Duke, R. Gasser, E. Greeley, A. Ochadlick, L. Ott, W. Payton, W. Schmidt) | 7 |
| NISC, Code 20 (G. Batts), Code 43 (J. Erdmann), Code OW17 (M. Koontz) | 3 |
| NOSC, Code 407 (C. Ramstedt) | 1 |
| NAVPGSCOL, Code 06 (R. Fossum) | 1 |
| U.S. Naval Academy/Annapolis (C. Schneider) | 1 |
| GTE Sylvania/Needham, MA (G. Pucillo, D. Esten, R. Warshamer, D. Boots, R. Row) | 5 |
| Lockheed/Palo Alto, CA (J. Reagan, W. Imhof, T. Larsen) | 3 |
| Lawrence Livermore Labs/Livermore, CA (J. Lytle, E. Miller, L. Martin) | 3 |
| Raytheon Co./Norwood, MA (J. deBettencourt) | 1 |
| U. Nebraska/Lincoln, NB (E. Bahar) | 1 |
| Newmont Exploration Ltd./Danbury, CT (A. Brant) | 1 |
| IITRI/Chicago, IL (J. Bridges) | 1 |
| Stanford U./Stanford, CA (F. Crawford) | 1 |
| U. Colorado/Boulder, CO (D. Chang) | 1 |
| SRI/Menlo Park, CA (L. Dolphin, Jr., A. Fraser-Smith, J. Chown, R. Honey, M. Morgan) | 5 |
| Colorado School of Mines/Golden, CO (R. Geyer, G. Keller) | 2 |
| U. Arizona/Tucson, AZ (D. Hastings) | 1 |
| U. Michigan/Ann Arbor, MI (R. Hiatt) | 1 |
| U. Washington/Seattle, WA (A. Ishimaru) | 1 |
| U. Wisconsin/Madison, WI (R. King) | 1 |
| U. Wyoming/Laramie, WY (J. Lindsay, Jr.) | 1 |
| U. Illinois/Urbana, IL (R. Mittra) | 1 |
| U. Kansas/Lawrence, KS (R. Moore) | 1 |

INITIAL DISTRIBUTION LIST (Cont'd)

| Addressee | No. of Copies |
|---|---|
| Washington State Univ./Pullman, WA (R. Olsen) | 1 |
| N. Carolina State Univ./Raleigh, NC (R. Rhodes) | 1 |
| Ohio State Univ./Columbus, OH (J. Richmond) | 1 |
| MIT Lincoln Lab./Lexington, MA (J. Ruze, D. White, J. Evans, A. Griffiths, L. Ricardi) | 5 |
| Purdue Univ./Lafayette, IN (W. Weeks) | 1 |
| U. Pennsylvania/Philadelphia, PA (R. Showers) | 1 |
| EB Div. General Dynamics/Groton, CT (R. Clark, L. Conklin, H. Hemond, G. McCue, D. Odryna) | 5 |
| Science Application Inc./McLean, VA (J. Czika) | 1 |
| JHU/APL, Silver Spring, MD (W. Chambers, P. Fueschel, L. Hart, H. Ko) | 4 |
| DTIC | 12 |